Joint inversion of MCS and OBS datasets for superior modelling: a case study from offshore NW Sumatra

Dibakar Ghosal, Indian Institute of Technology Kanpur, Kanpur 208016, U.P., India*
Ajay P. S. Chauhan, British petroleum
Satish C. Singh, Institut de Physique du Globe de Paris, Jussieu, 75014, Paris, France

**dghosal@iitk.ac.in*

Keywords

Tomography, Joint inversion, Pre-stack depth migration, OBS, MCS

Summary

Velocity-depth modelling using conventional normal move-out (NMO) analysis in a complex geologic setting is very challenging. Additionally, refraction arrivals associated with the low sediment velocities and deep water only appear at far offsets, containing information about deeper structures. In this study, we therefore present an innovative method where a 12 km long towed, downward continued streamer seismic data and the ocean bottom seismometer data are jointly inverted to determine a high-resolution near surface velocity-depth model. The quality of the inverted velocity is then justified performing a pre-stack depth migration using the streamer data. Our findings infer that the velocity-depth model derived from jointly inverted tomography study produces a detail pre-stack depth migrated image.

Introduction

Imaging of subsurface geology, using conventional NMO based technique, is very challenging in a complex geological setting like an accretionary wedge deposits associated with the subduction zones e.g. Sumatra (Singh *et al*., 2012) where the water depth may vary from a couple of meters to several kilometers across the subduction front. Thus, redatuming techniques are explored (Ghosal *et al*., 2014, Ghosal *et al*., 2017) to enhance refracted phases for superior modeling. Here, we present a novel technique, in which we have carried out a joint inversion of the multi-channel seismic datasets (MCS) and ocean bottom seismometer (OBS) recorded datasets, which were acquired coincidentally offshore northern Sumatra in 2006 (Figure 1) using the French R/V Marion Dufresne and the Western Geco M/V *Geco Searcher* vessel carrying 8260 cu in. and 10170 cu in. airgun array sources, respectively in July–August 2006. The 520 km-long WG2 profile (Figure 1) is orientated $\sim 20^0$ anticlockwise from the trench normal on which 56 ocean-bottom seismometers (OBS) spaced at 8.1 km were deployed and shots were fired at 150 m intervals. A 12-km-long streamer towed at 15 m depth was used for the reflection survey at 50 m shot interval, to image the deeper structure of the megathrust (Singh *et al*., 2008).

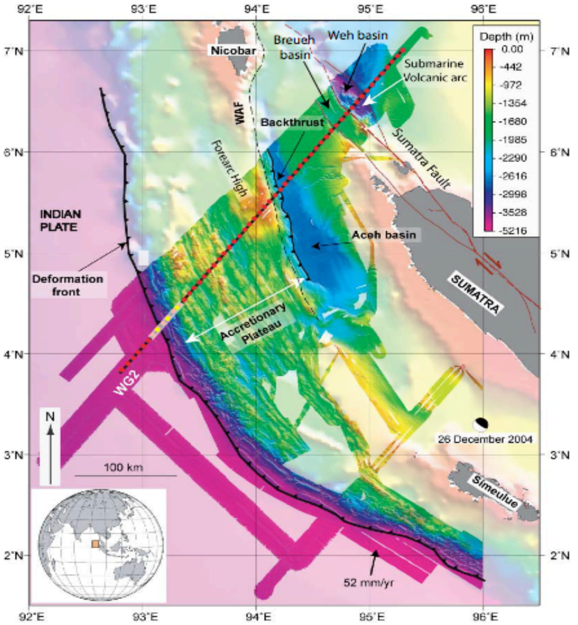

Figure 1: Location of seismic reflection profile WG2 superimposed on bathymetric data. Red dots: OBS locations; Solid Black line indicates the WG2 profile. White line segment is imaged in figure 5.

Theory and/or Method

(i) Background to joint inversion

An example of an OBS gather is shown in figure 2. The travel time inversion for only the OBS datasets (Figure 2) (Chauhan *et al*., 2009; Chauhan, 2010; Singh *et al*., 2012) was carried out using an adaptive parameterization approach where the minimum triangulated grids were fixed to 1.25 km spacing. The horizontal and vertical smoothing parameters for the inversion were set to 15 km and 2 km, respectively, which ultimately provided a smooth velocity model having a resolution in a scale of tens of kilometres (Figure 4a). Later on, the resulting velocity model was used as the background model for the tomographic analysis of a 12 km long streamer, which was downward continued to seafloor (Berryhill, 1979; Ghosal *et al*., 2012, 2014). During inversion a 50 m square grids were chosen to discretize the models; the ratio of the regularization parameters was selected along horizontal and vertical directions as 1:4. The overall resolution of these models resulted in a scale of several hundred meters (Ghosal *et al*., 2012, 2014).

Since the grid dimensions and regularization parameters are very different for the OBS and MCS data inversion independently, integration of the best fit models from these methods using the common interpolation methods may produce significant discontinuities at the model boundaries. To get rid of such difficulties, we have jointly inverted the first arrival travel times of the OBS and downward continued MCS datasets. The crux of the parameterization for the joint inversion is described in the following section.

(ii) Joint inversion of OBS and MCS data

In the joint inversion scheme, the model parameterization is a crucial component. The grid spacing for the joint inversion was chosen as 100 m which is 2 times larger than the shot interval maintained in MCS data inversion and less than OBS data inversion described in earlier section. The model length and the depth were kept similar to the previous OBS tomography work to make easy the later comparisons.

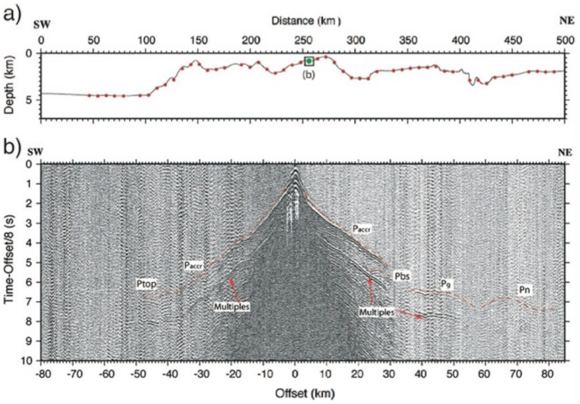

Figure 2: (a) Bathymetry along the OBS profile. Red circles- OBS positions; green circle- the position of OBS data. (b) OBS data. Brown dash- main arrivals. Paccr: P-wave in accretionary sediments, Ptop: Reflection from the top of the oceanic crust, Pbs: Reflection from the back thrust, Pg: Crustal arrival, Pn: mantle arrival (figure adapted from Singh *et al*., 2012).

The travel time picks for MCS datasets were done using a semi-automatic technique, and the travel time picks for the OBS datasets (Figure 2) are adapted from the previous work done by Chauhan, (2010). Since the total travel time picks for the MCS datasets were nearly 1.2 million and for OBS datasets were having travel time picks of 30,000; therefore, we had to reduce these discrepancies using the travel times for every 8th shot gather for MCS datasets and all the travel time picks from the OBS datasets. In such a way, the total used travel time picks for the joint inversion becomes nearly 620,0000.

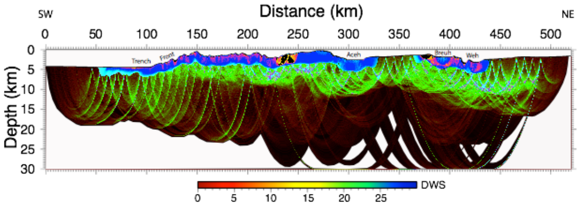

Figure 3: Derivative weight sum (DWS) plot for the OBS profile. The shallow section is illuminated by the dense MCS rayfans (blue part), whereas the deeper part is mainly sampled by the OBS rayfans.

Since both types of travel time picks are merged together, the rays travel through both shallow sections and deeper sections simultaneously. Shallow sections are sampled densely by the MCS datasets and partly by the OBS datasets, whereas the deeper sections are primarily covered by the OBS datasets (Figure 3). The rayfans sample the trench deposits to a depth of nearly 18 km and the ray density gradually increases northeastward and it reaches its maximum (nearly 30 km) below the forearc high. The ray density suddenly falls below the Sumatra platform and becomes high again below the Breueh and Weh basins.

The inversion is carried out using the same tomographic package (Van Avendonk *et al.*, 2004) that was used earlier for the MCS datasets. The starting model was chosen as the initial model from Chauhan, (2010). The initial misfit was 300 ms, which has been reduced gradually to 5 ms after 17th iteration. The reduction in the travel time misfit was calculated using the chi square value.

(iii) Pre-stack depth migration

The interval velocity, which is required as the input for pre-stack depth migration, was obtained from the travel time tomography of jointly inverted datasets. We have used the 12 km long streamer data, for pre-stack depth migration wherein sampling interval was kept as 2 ms, in order to obtain high-resolution image in addition pre-processing steps were applied to remove swell noise attenuation and multiples. Apart from this we have also applied inner trace mute on these data to effectively suppress the existing residual multiples from the near offset. Effect of side scattering is reduced by applying dip filtering. Moreover, a mild triangular anti-aliased filter was used.

Examples (Optional)

Figure 4 demonstrate the starting (figure 4a) and the OBS inverted model (figure 4b) and joint inverted model (figure 4c), respectively. It is clear that the small wavelength structures in the shallow section of the best-fit model (Figure 4c) were improved after the inversion in comparison to the earlier OBS data inversion only (Figure 4b). In the subduction front, the high velocity layers proceed upward close to the seafloor; below the Aceh basin a significant velocity change is observed. The high velocity contours appear close to the basin representing the presence of strong basement materials. The recovery of the small wavelength structures was also found beneath Breueh basin. The right hand flank of the Great Sumatran Fault is also mapped here (Ghosal *et al.*, 2012) and further northeast the Weh basin bounding normal faults are also resolved. All these small wavelength features were missing in the images reported by Chauhan, (2010), but due to the joint inversion we can recover these features in our best-fit model with the presence of the long wavelength structures at depth.

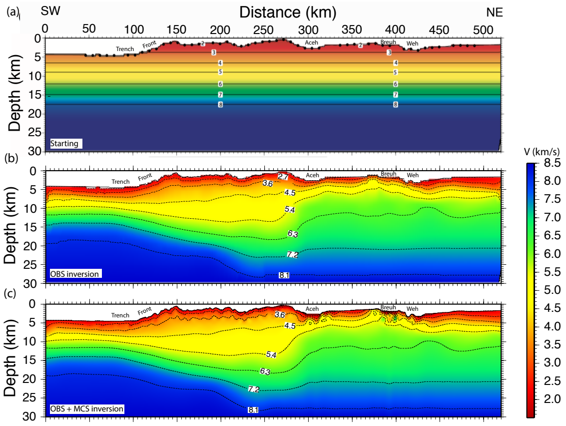

Figure 4: (a) Starting model; (b) OBS data inverted model adapted from Chauhan, (2010); (c) best-fit model after joint inversion of OBS and MCS data.

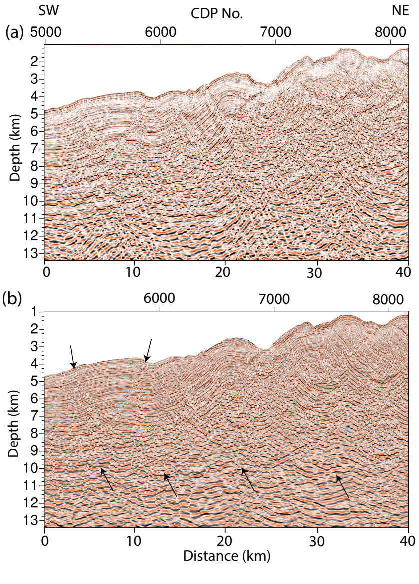

Figure 5: (a) Depth converted image using OBS tomography result only (Chauhan, 2010) and (b) prestack depth migrated image implementing the jointly inverted velocity.

Figure 5a illustrates a subset of the depth converted result below the oceanic deposits, subduction front and outer accretionary plateau (Figure 1). Although the shallow structures are more or less clear from this image, the plate geometry is difficult to interpret clearly due to the improper velocity. To improve the image quality, we have used our jointly inverted best-fit velocity-depth model for the pre-stack depth migration. Figure 5b shows an example of the pre-stack depth migrated section of the same subset of WG2 profile shown in Figure 5a. One can clearly observe significant improvement of the near surface and deep crustal structures in the depth migrated image. The bi-vergent faults are more prominent and the top of the oceanic plate and are imaged well in the depth migrated section.

Conclusions

Based on the joint inversion results we draw the following conclusions:

1) The jointly inverted velocity-depth model is well constrained in the shallow section and yields information at depth as well and will be immensely useful for future work. This velocity-depth model provides the complete picture of the velocity distribution of the Northern Sumatra subduction setting.

2) The pre-stack depth migrated result, using the jointly inverted best-fit model, provides detail image of both shallow and deeper structures.

References

Berryhill, J.R., 1979, Wave equation datuming, *Geophysics,* **44,** 1329–1344.

Chauhan, A. P. S., S. C. Singh, N. D. Hananto, H. Carton, F. Klingelhoefer, J. Dessa, H. Permana, N. J. White, and D. Graindorge, 2009. Seismic imaging of forearc backthrusts at northern Sumatra subduction zone, Geop. Journal International, 179, 1772-1780

Chauhan, A. P. S., 2010. Structure of the Northern Sumatra subduction megathrust using seismic reflection and refraction data, Institut de Physique du Globe de Paris, PhD Thesis

Ghosal, D., Singh, S.C., Chauhan, A.P.S. & Hananto, N., 2012, New insights on the offshore extension of the Great Sumatran fault, NW Sumatra, from marine geophysical studies, *Geochem. Geophys. Geosyst.,* **13,** doi:10.1029/2012GC004122.

Ghosal, D., S.C. Singh, J. Martin, 2014, Shallow subsurface morphtectonics of the NW offshore northern Sumatra subduction system using an integrated seismic imaging technique, *J. Geophys. Res.*, 198, 1818-1831, doi: 10.1093/gji/ggu182.

Singh, S.C., H. Carton, P. Tapponnier, N. Hananto, A.P.S. Chauhan, D. Hartoyo, M. Bayly, S. Moeljopranoto, T. Bunting, P. Christie, H. Lubis, J. Martin, 2008, Seismic evidence for broken oceanic crust in the 2004 Sumatra earthquake epicentral region, *Nat. Geosci.,* 1, 771–781.

Singh, S. C., Chauhan A. P. S., Calvert, A. J., Hananto, N. D., Ghosal, D., Rai, A., Carton, H., 2012. Seis-mic evidence of bending and unbending of subducting oceanic crust and the presence of mantle megathrust in the 2004 Great Sumatra earthquake rupture zone, Earth Planet. Sci. Lett., 321-322, 166-176, doi:10.1016/j.epsl.2012.01.012.

Van Avendonk H.J.A., D. Shillington, W.S. Holbrook, M. Hornbach, 2004, Inferring crustal structure in the Aleutian island arc from a sparse wide-angle seismic data set, *Geochemistry Geophysics Geosystems*, 5, 8, 1527-2087.

Acknowledgments (Optional)

We are thankful to A. Harding, N. Bangs, H. Carton, N. D. Hananto for their support during this study. We are grateful to Western Geco for carrying out the survey for us.